JREE: Vol. 5, No. 2, (Spring 2018) 22-30

Journal of Renewable Energy and Environment

Research Article

Journal Homepage: www.jree.ir

Experimental Investigation of the Efficiency of a Semi-Spherical Solar Piping Collector

Mojtaba Moravej*, Fatemeh Namdarnia

Department of Mechanical Engineering, Payame Noor University, Iran.

PAPER INFO

Paper history:
Received 06 February 2019
Accepted in revised form 09 April 2019

Keywords:
Semispherical Solar Collector
Received Radiation
Efficiency
Different Flow Rate

ABSTRACT

Solar water heaters are good tools for saving fuel. The main component of these water heaters is collectors, which are responsible for absorbing solar energy and transferring it to the working fluid with the least heat dissipation. The present study is an experimental study of the performance of the solar semispherical collector with 1 m^2 of absorber area at different volumetric flow rates. Water was used as the working fluid with the volumetric flow rate between 0.005-0.0166 kg/s, and the experiment was conducted in the ASHRAE 93 standard conditions. The results showed that the efficiency of semispherical solar collector increased as the flow rate of the working fluid increased, such that the highest efficiency, which is 67 %, belonged to mass flow rate 0.0166 kg/s. In addition, the difference between outlet and inlet temperatures decreased due to the system being closed during the test. In addition, according to the experiments, the reduction of radiation and wind speed did not have any significant effect on the efficiency and outlet temperature of the collector. Finally, parameters such as inlet and outlet temperature of collector, ambient temperature, ambient radiation intensity and their effect have been investigated empirically on the collector efficiency graph.

1. INTRODUCTION

In Iran, on average, there are 280 sunny days as reported annually, which is very significant. In the present day, solar energy is used for various uses [1]:

- Use of solar thermal energy for household, industrial, and power use (Heat sink).
- Direct conversion of solar beams into electricity by equipment called photovoltaic (Solar Power).

These systems generally consist of a solar radiation collector, working fluid, a storage tank, a pump, piping unit, and auxiliary heating unit [2, 3]. Stationary collectors such as flat plate collectors are the most common type of solar collectors usually used as a water or air heater. These types of collectors have low efficiency and low outlet temperature [4-8]. The most important factor in solar water heating is efficiency. The efficiency of a solar water heating system depends on the ratio of the received useful energy from the heated water to solar irradiance [9]. Solar collector properties play an important role in efficiency value [10]. Scientists and engineers are seeking new ways to increase efficiency in order to increase the performance and decrease the expenses. The absorbent surface of solar collector is very effective in the efficiency value. The absorber color, configuration factor, and the heat transfer between the absorbent and working fluid are of extreme importance [11, 12] and should be investigated widely. These studies proposed the application of gas particle suspension [13], fluid-film [14], and metal foam [15] to increase this heat transfer. Another factor that plays an important role in efficiency of solar collector is working fluid. There have been many experiments in this field [16-19]. An experimental study of the effect of Cu-synthesized/EG nanofluid on the efficiency of flat-plate solar collectors is one of them that was carried out by Zamzamian et al. [20]. They figured out that by increasing the nanoparticle weight fraction, the efficiency of the collector could be improved. In addition, they discovered that the lowest removed energy parameter could be reached by using 0.3 % Cu/EG nanofluid at 1.5 l/min and the highest absorbed energy parameter was achieved under the same conditions. Jamal-Abad et al. [21] studied the performance of a flat-plate collector by using Cu-Water nanofluid in an experimental research. They found that the collector efficiency was higher when the concentration of nanoparticles was raised. The results also revealed that the efficiency of the collector at 0.05 wt% was approximately 24 % more than that the pure base fluids in the same conditions. Their study confirmed that nanofluids had considerable potential for solar collectors. Another method for increasing the collector's performance is increasing the collector ability to absorb all parts of sun radiation. One way is using solar tracking mechanism that can increase the yearly solar radiation gain up to 1.45 times more than an optimal tilted solar collector [22]. Other way is using suitable and symmetric surfaces such as spherical or conical. The conical solar collector was investigated by Noghrehabadi et al. [23]. The results of the experiments indicated that the performance of conical collector increased greatly, contrary to flow rate growth. This improvement in efficiency results from a specific shape that absorbs all parts of sun radiation and the centrifugal forces with a secondary flow generated by longitudinal vortices. Another important conclusion of this article is that the maximum temperature and efficiency of the present conical collector were about 77.1 ^oC and 60 %, respectively, and pressure drop via conical collector was more than 5 kPa. Oztekin Bakir [24] in an experimental analytical study built a solar spherical collector, whose reservoir of water with a capacity of 130 liters was devised within the collector. It consists of a spherical body with a 1m^2 absorber plate and

*Corresponding Author's Email: moravej60@pnu.ac.ir (M. Moravej)

0.68 m diameter, a glass cover made of silicon in the form of two half-cores and working fluid. During each experiment, local temperatures on the absorber surface and on the cover surface, water temperature at collector inlet, and collector outlet, ambient temperature, and solar radiation intensity were measured and recorded with a time interval of 15 minutes. He tested this collector in two fluid-free and with fluid condition with masses of 0.002, 0.005, 0.007, and 0.11 and compared the results with those of testing two flat collectors with areas of 0.28 and 56.02 square meters. It is seen in the figures that hourly efficiencies of the spherical solar collector are greater than those of the flat plate collectors under these experimental conditions ($T_f \leq 34.4$ °C), T_f is the water temperature within the spherical collector. In addition, an increase in the hourly efficiency is greater for the spherical collector throughout the day. Although there is a decrease in the hourly efficiencies of the flat plate collectors in the afternoon, hourly efficiency of the spherical collector shows an increasing pattern. Maximum hourly efficiency obtained for the flat plate collectors of 0.28 m^2 in area and 0.56 m^2 in area are 56 % and 55 %, respectively. Maximum hourly efficiency obtained for the spherical collector is 79 %. He also observed in this experiment that half of the sphere is always exposed to the sun and receives radiation; as a result, it has come to the conclusion that the use of a light reflector can be effective in a shadowy area. It also concluded that the use of two glass covers or a thicker glass cover could be more effective in reducing heat dissipation. In a computational work, Pelece et al. [25] calculated the energy generated by a semispherical solar collector with an area of one square meter and compared it with the amount of energy obtained by the flat plate solar collector, which, according to the results obtained, the energy produced by semispherical collector is 1.3 times larger than the flat collector when placed at an optimal slope and 1.6 times larger than the energy obtained by the flat collector when horizontally placed. In a laboratory study, Pelece et al. [26] also studied the performance of a semispherical collector without reflecting light and using a light reflector. The reason for this experiment is that although the semispherical solar collector receives solar energy from all directions and that there is no point on it that does not receive direct radiation energy [27], the northern receives direct radiation only in the morning and in the afternoon; in the middle of the day, its temperature is significantly lower than that in the south. In this experiment, they used a flat reflector with dimensions of 6×3 m and a reflection coefficient of 0.6, which allowed the reflector to receive a greater energy of 1.6 times. They also concluded that it was not necessary to raise the collector to the top of the roof; however, the collector could be located next to the southern wall of the building, and the reflector was installed on the wall. Volumetric and mass flow rates have an impact on the performance of solar collectors. Different flow rates cause different efficiencies. Accordingly, choosing the optimum flow rate in every collector should be considered as one of the significant factors in selecting and using the collectors. There are many studies about the effect of flow rate on collector's efficiency. Yousefi et al. [28] investigated three flow rates for flat plate collector, and showed that the efficiency of collector increased as the mass flow rate increased. Mintsa et al. [29] conducted a research on polymer flat plate collectors, and revealed that by increasing the flow rate, the performance of the collector would increase; these results are similar to experimental work of Cristofari [30]. In the present study, the performance of a semispherical collector as a stationary and symmetric solar collector is investigated at different flow rates. One of the most important features of these collectors is the ability to absorb diffuse and direct radiation simultaneously. One of the other benefits of this kind of collectors is that there is no need for following up the sun, navigation, and easy maintenance and repair. Because of its spherical shape, all of the geographic directions have the same effect, and because of its semi-spherical shape during the day, some of the surface is under direct radiation. In addition to its spherical shape, it exhibits the highest stability and disruption to the wind.

The main advantage of the semi-spherical solar collector is its ability to collect solar energy from all sides to conform to the long path of the Sun in the summer. Actually, there are no spots on the semi-spherical absorber, which would not receive the solar beam radiation. In order to achieve the efficiency of semispherical solar collector, the water as a working fluid passes through the collector and the heat is transferred from collector to water. The collector efficiency is the ratio between transferred heat from the collector to the working fluid and the amount of the received solar energy by the collector.

This collector is tested in a closed circuit. Contrary to what has been done so far, the flow temperature of the inlet to the collector has not been taken into account with the same ambient temperature, and the actual results of the experiments have been used. In this paper, parameters such as inlet and outlet flow temperature, ambient temperature, ambient radiation intensity, and their effect on collector efficiency graph are investigated empirically, and collector efficiency charts are plotted. In the experiments, the effect of the parameter of the mass flow rate has also been studied.

2. MATERIALS AND METHOD

2.1. Governing Equation

The useful energy gained by the fluid passing through the collector is [31]:

$$Q_u = \dot{m} C_p (T_{out} - T_{in}) \quad (1)$$

where T_{in} and T_{out} are the temperatures of the inlet and outlet of the fluid from the collector, respectively, and C_P and $\dot{m}$ represent the specific heat and mass flow rate of the fluid, respectively [31].

The useful energy obtained by the collector in terms of the amount of solar radiation input and the heat loss of the collector body is [31]:

$$Q_u = A_p F_R [S - U_l (T_{in} - T_a)] \quad (2)$$

In the above relation, T_a is the ambient temperature, A_P is the surface area of the absorber, and F_R is the heat removal coefficient, which is defined as follows [31]:

$$F_R = \frac{\dot{m} C_p}{U_l A_p} [1 - \exp(-F' U_l A_p / \dot{m} C_p)] \quad (3)$$

S is part of the solar radiation absorbed by the collector absorber surface area. S is obtained through the following equation [31]:

$$S = (\tau\alpha) I_T = \eta_o I_T \quad (4)$$

where the solar flux, I_T, is added to the collector, η_o is the optical efficiency and is an effective product of cross-absorption obtained through the following relationship [31]:

$$\eta_o = (\tau\alpha) = 1.01\tau\alpha \quad (5)$$

In steady state, the useful energy received by the collector is:

$$Q_u = A_p S - U_l A_p (T_p - T_a) \quad (6)$$

where T_p is the absorbent plate temperature, and U_l is the overall drop from the collector [31]. Since the solar meter shows total radiation, it is required to find a way to calculate the total energy absorbed by the collector. The surface of semispherical collector in this experiment is divided into 12 slices. In order to obtain the total amount of received radiation, the radiation received by each of the slices should be calculated. Because the area of each slice is the same, the total amount of received radiation from the multiplication of the area of each of slice by the amount of received radiation by the solar meter can be calculated [31].

$$\sum A_{Pi} . I_{Ti} = A_{P1} I_{T1} + A_{P2} I_{T2} + \cdots A_{P12} I_{T12} \quad (7)$$

Now, by means of the data obtained from testing every 30 minutes including the temperature of the inlet and outlet water, the ambient temperature, the intensity of the received radiation, and placement in equation (8), the collector's efficiency was calculated every 30 minutes. Factors affecting the rate of efficiency include the mass flow rate, the difference between the temperatures of the outlet and the input water, and the total received radiation intensity, which here are used in the analysis [32].

$$\eta = \dot{m}c(T_{out} - T_{in}) / \sum I_T A_P \quad (8)$$

where $\dot{m}$ is the mass flow rate, T_{out} is the temperature of the outlet water, T_{in} is the input water temperature, and I_T A_P is the intensity of the radiation received by the hemisphere.

2.2. Materials

The experiments were carried out in winter at the Behbahan city in the south of Iran (latitude is 30° 36' 0" N and longitude is 50° 14' 0" E). The characteristics of solar semispherical collector used in this experimental test are given in Table 1. The solar semispherical collector used in this work is made by the authors in Payame Noor University, Iran (Figure 1). Experiments were performed with different flow rates of 0.005, 0.108, 0.0133, 0.0126, and 0.0166 kg/s. Each flow rate was tested several times, and the data of the tables include the average of the data. The wind speed was measured from 0.2 to 8.2 m/s on the test days. During the experiment, ambient temperature, temperatures of collector absorber surface and collector glass surface, and inlet and outlet water were measured by thermocouples (type K), and these sensors were connected to a channel data logger (TES data logger model). The solar radiation was recorded by a solar meter, also these measures are recorded at a time interval of 30 minutes. The measurement tolls are shown in Figure 2.

3. TESTING METHOD

ASHRAE Standard 86-93 for testing the thermal performance of collector is certainly used most often to evaluate the performance of stationary solar collectors [33] (shown in Table 2). The thermal performance of the solar collector is determined by obtaining the values of instantaneous efficiency for different combinations of incident radiation, ambient temperature, and inlet fluid temperature [34, 35] (Figure 3). According to ASHRAE Standard 86-93, steady-state conditions should be prepared during the data period and, also, during a specific time interval prior to the data period, which is called pre-data period. Reaching steady-state variables must be in a specific limitation, as defined in Table 3, in the entire test period. The standard according to which these experiments were carried out is the ASHRAE 93 standard whose general conditions are listed in the Table 2 [33].

3.1. Description of Device Calibration

Calibration of measuring instruments were undertaken before, during, and after the experimental data collection. Thermocouples were calibrated by using an independently calibrated platinum resistance thermometer; flow meter used a data-logging sub-routine to draw water from the systems into a container and measuring the mass with accuracy scales, and solar meter used a calibrated reference solar meter with a valid calibration certificate. The accuracy of thermometer data logger is 0.1 and accuracy of flow meter is 0.05 kg/min. Tracking of total solar radiation was implemented by a TES 132 solar meter type with an accuracy rate of 1 w/m^2.

3.2. Error Analysis

Due to ASME guidelines, there are no absolute measurements and errors in any experimental measurement. Some of the usual sources of error include the errors of calibration, data recording errors, and inappropriate instruments [36-37]. Errors in flow rate measurement, temperature measurement, and solar radiation measurement are the main components in uncertainty in collector efficiency. The uncertainty results of the measurement including all the sources of errors are shown in Table 3. In measuring any quantity, we usually repeat each measurement several times in exactly the same conditions with a definite device. This action reduces some of the error factors. The average value of the measured values is the best and most likely value of the quantity. The combined uncertainty for calculating the collector efficiency, Sη, was determined by the root sum square method (RSS) based on Equation (8) [38]. This analysis is done through equation (9). It is assumed that errors in C_P and A_C are negligible.

$$\int S\eta = \sqrt{\left(\frac{\Delta m}{m}\right)^2 + \left(\frac{\Delta G}{G}\right)^2 + \left(\frac{\Delta(\Delta T)}{\Delta T}\right)^2} \quad (9)$$

where $\Delta m/m$ is the flow rate changes, $\Delta G/G$ represents the received radiation changes, and $\Delta(\Delta T)/\Delta T$ is used to measure variations in the temperature of the inlet and outlet of the working fluid. The maximum uncertainty determined in the present work in calculation of the collector efficiency based on several tests was about 6%.

Table 1. The characteristics of semispherical solar collector.

Characteristics		Dimension	Unit
Coverage	• Glass radius A transparent glass sheet with a thickness of 6 mm was installed as a cover on the metal, which allows the passage of light, yet reduces the loss of heat transfer by stacking the air between the absorber and the glass and reduces heat dissipation. • Conducting • Density • Specific heat • Reflection coefficient • Absorption coefficient • Dispersion coefficient	43 12.1 2200 670 0794.0 0386.0 526.1	cm w/m.c° g/cm^3 J/kg.c°
Absorber	• Absorbent radius A high-temperature thermal conductive absorber made of iron and its surface is darkened by the use of a bluish black color, which absorbs solar energy better. The thickness of the sheet metal is 3 millimeters. • Conducting • Specific heat • Density • Type of absorbent coating • Absorption coefficient	39 4.80 10.25 87.37 Opaque black color 9.0	cm w/m.c° J/kg.c° g/cm^3
Tubes	Copper tubes soldered to the absorbent surface and the fluid inside the tubes receives heat from the absorber. The diameter of these pipes is 3.8 inches.	3.8	
Working fluid	• A heat transfer fluid which is water in this experiment that absorbs heat from the absorbent surface. • Specific heat capacity • Density		J/kg.c° g/cm^3
Insulation	• A heat insulator placed under the collector and has a thickness of 2 centimeters. It is usually made of plastophome, which reduces heat dissipation. • Insulating glass wool 2 centimeters thick, wrapped around the metal beneath the collector to prevent heat loss by the collector's below metal surface. • Insulation tank • A domestic water purifier pump for pumping water inside the reservoir into the collector.		

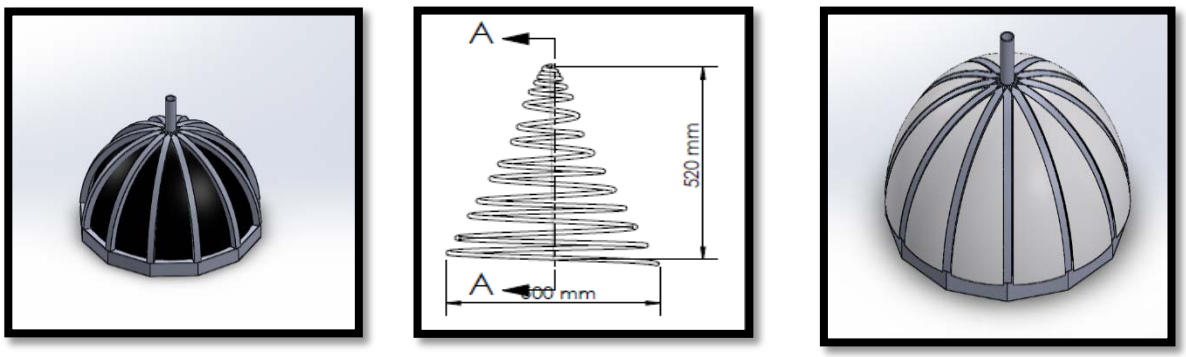

Figure 1. Absorber and glass cover surface and piping in a semispherical solar collector.

Figure 2. TES data logger model, solar meter, and thermocouples (type K).

Table 2. Standard test conditions (ASHRAE 93).

Parameter	Unit	ASHRAE 93
Accuracy of temperature cold water inlet	°C	± 1
Accuracy of temperature difference across hot water system	°K	± 0.5 (°C)
Precision of temperature difference across hot water system	°K	± 0.2 (°C)
Ambient air temperature position	---	At a distance of 1.2 m above the ground and at a minimum distance of 1.5 m from the reservoir and the system
Pipe length	M	15
Pyranometer	---	Class I
Accuracy of temperature ambient air	°C	± 0.5
Precision of temperature ambient air	°C	± 0.2
Accuracy of the liquid flow rate measurement	% mass per unit time	± 1
Mass measurement	%	± 1

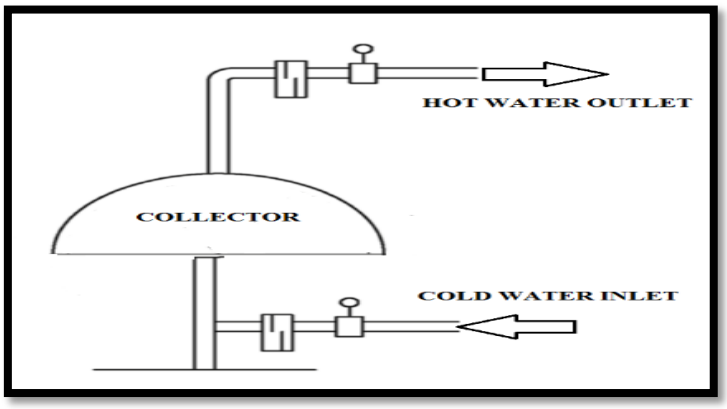

Figure 3. Schematic view of the experimental setup.

Table 3. Results of uncertainty in the present work.

Parameter	Uncertainty (%)
Volumetric flow rate	±0.5
Solar radiation	±5
Difference between inlet-outlet temperature	±1.1

4. RESULTS AND DISCUSSION

In the next sections, the application of the experimental results, performance, temperatures variation, and effect of volumetric flow rates in the semi-spherical solar collector will be analyzed. All data are tested in a quasi-steady state condition. The collector is perpendicular to the ground and water is used as working fluid. The tests of the collector were conducted during several days in winter 2017, which were carried out during the day from 8:00 to 16:00 o'clock. The data were logged every 30 minutes. Figure 4 presents the solar radiation and temperature profiles in one the test days. In this figure, sun radiation and key temperature of a selective day versus local time are shown. It is clear that the maximum received radiation is near the solar noon. In this diagram, radiation rates are lower in the early hours of the day and, as the noon approaches, it increases and decreases around the

evening, except during cloudy days; the radiation rate may reduce at noon due to cloudiness of the air. In all days, since the test system is a closed system, the inlet water temperature increases gradually. In all days, the outlet temperature has increased with time around noon, and even if the radiation rate is reduced as a result of reduction of direct sunlight, the graph of the temperature of the outlet water shows an increase, which indicates that this collector using a 6-mm glass cover keeps the absorbed heat well and, also, demonstrates the capability of this type of collector in absorbing indirect radiation, which includes reflection and reflection [39].

Total radiation received by the collector according to Equation (10):

$$I = I_{BC} + I_{DC} + I_{RC} \quad (10)$$

where I_{BC} is the amount of radiation received directly, I_{DC} is the diffused radiation and I_{RC} is the radiation reflected from the surrounding objects. Figure 5 shows that the temperature of the inlet water is constantly changing over time and increasing, because the tested system is a closed system. Considering the fact that there is a sudden drop in radiation rate at the end of the day as approaching the sunset, an ascending pattern in outlet water temperature is observed. The analysis of Figure 6 shows that due to an increase in received radiation, the inlet and outlet water temperatures increase. With the passage of time and approaching the evening, charts tend to maintain their ascendancy and increase. The factors affecting the maintenance of an increase in the temperature of the outlet water include the absorption of radiation from all sides of collector and a 6-mm glass cover, which imprisons the air between the absorbent and the coating and prevents its dissipation. Effective factors in efficiency are mass flow rate, difference between the output and input water temperatures, and received radiation. By drawing the corresponding diagrams, the effect of each parameter on the efficiency has been determined. A review of the efficiency graph is presented in terms of mass flow rate; greater mass and its impact will be more effective in increasing efficiency.

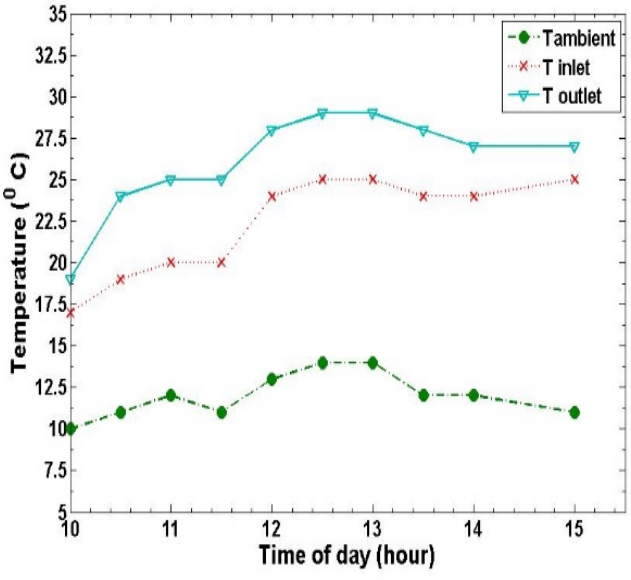

Figure 4. Changes in inlet and outlet water temperatures, received radiation, and ambient temperature on a test day.

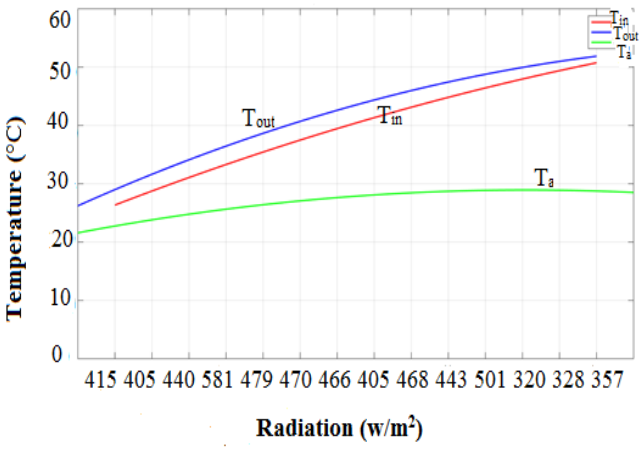

Figure 5. Changes in inlet and outlet water temperature and ambient temperature in terms of radiation.

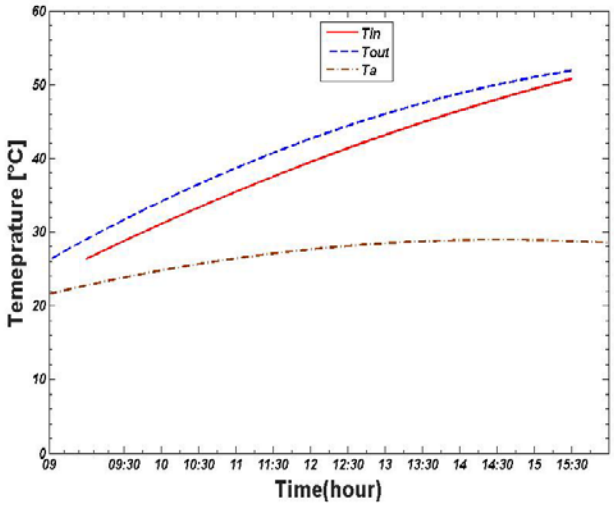

Figure 6. Changes in the output and inlet temperature and the ambient temperature in time.

Figure 7 shows a comparison of the efficiency with different flow rates, and as is clear from the charts particularly in Chart 7, at all times of the day, the graph has greater mass than the graph with lower mass flow. Figure 8 shows that the volumetric flow rate has a non-linear effect on the performance of the solar semispherical collector. According to this figure, the volumetric flow rate that produces the best efficiency is at its highest level, and the maximum value of efficiency in this work is about 67 %, while these values for flat plate collectors in studies of Jamal-Abad et al. [21] and Yousefi et al. [28] were about 55 % and 54 %, respectively. By increasing the flow rate, the efficiency inclines to an asymptotic value. This pattern shows that as the Reynolds number increases, the efficiency also increases. In addition, heat transfer increases due to the increasing Reynolds number, because the secondary flow causes the convectional heat transfer to increase [40, 41]. Figure 9 also reviews the collector efficiency according to the received radiation, which is seen as a result of increased radiation; in this regard, the efficiency increases; however, the efficiency may not increase in places with increased radiation due to the high heat dissipation in the radiation. With the increasing radiation, the amount of heat dissipation inside the collector increases, because all the radiation received is not transmitted to the fluid.

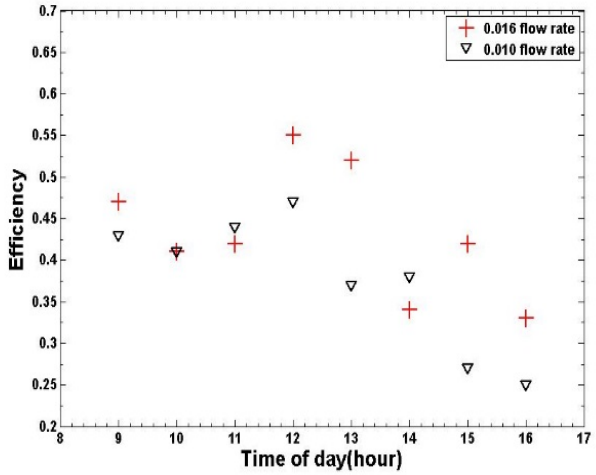

Figure 7. Collector efficiency based on different mass flow rates.

Figure 10 shows changes in the direction of the sun. During the day, parts of the collector are in the shadows and other parts in the direction of the sun. Due to the recording of thermocouple data on all 12 absorbent slices, the temperature of each slide is recorded and shown every 30 minutes. By using these data, Figure 10 is plotted and represents a change in the direction of the sun, and the temperature of absorber towards and behind the sun is also displayed at a time interval of 30 minutes.

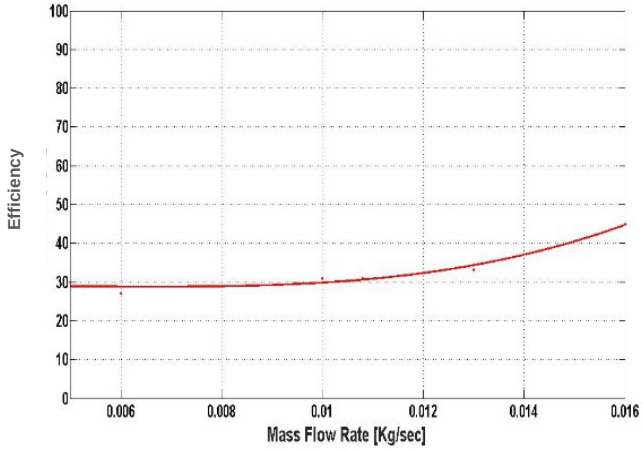

Figure 8. Collector efficiency based on different mass flow rates.

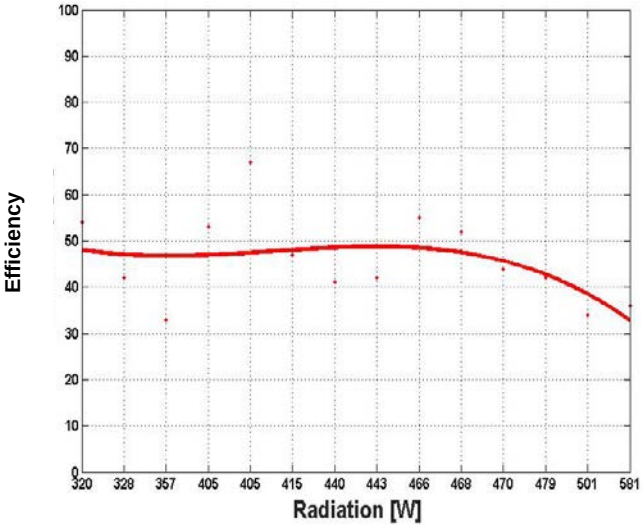

Figure 9. Changes in efficiency based on received radiation.

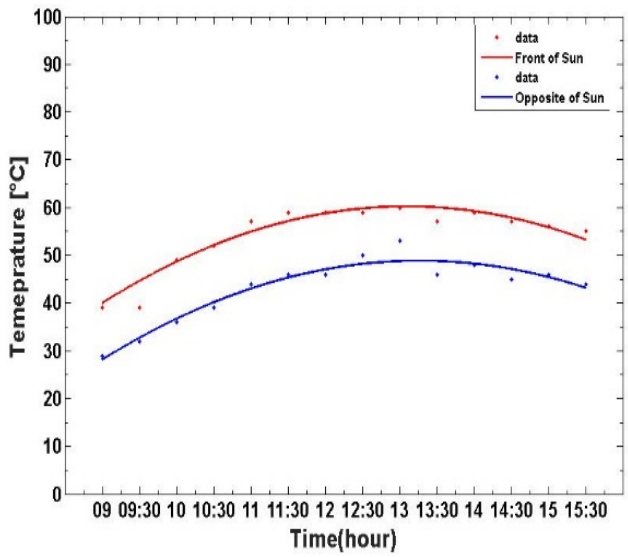

Figure 10. Display the temperature of the area facing the sun and back to sun.

5. CONCLUSIONS

In this research, the effect of different volumetric flow rates on the efficiency of a new stationary solar collector with a spherical geometry was experimentally investigated. To evaluate the volumetric flow rate effect, six values of flow rate between 0.005-0.0166 kg/s in a spherical collector with 1 m^2 of absorber plate and 0.6 m diameter were used. The total incident of sun radiation on the spherical collector was experimentally measured by 12 semi-flat absorbent slices. The results show that the performance of a spherical collector has increased greatly as opposed to flow rate growth. This improvement in efficiency results from the specific shape that absorbs all parts of the sun radiation. According to the aforementioned results, solar spherical collector can be used as a suitable water heater. When the high temperature value in outlet is required, the flow rate should be low; when the collector's high efficiency is required, the flow rate should be high.

As time passes, radiation increases and the output fluid temperature also increases gradually; as a result, the generated energy will be higher and, at noon, we have the highest amount of radiation; this amount will reach its maximum.

By reducing the flow rate of the fluid passing through the collector, the amount of energy received by the fluid increases so that the highest temperature of the outlet water belongs to the fluid with a flow rate of 0.055, which is about 53 degrees Celsius.

The temperature of the output water is shown in the diagrams whose output water temperature graph is ascending; even after the intensity of the radiation reduces and its graph pattern descends, the water output temperature will increase again. In fact, given the fact that the discussed semispherical collector was also tested in the winter, the sun's rays are not perpendicular to those in the summer, which covers the entire sphere. Due to the presence of glow in the winter in the testing hours, one third of the collector (usually four slices) was always in the direction of radiation, which is the reason why it is even close to sunset hours on the hemisphere. It is the reason for the justification of this type of collector.

In charts that exhibit the efficiency on different testing days, it was observed that the highest efficiency was 67 %, which

belonged to the highest mass flow rate of 0.166 and the smallest belonged to the smallest flow of mass, which is 0.055 and indicates that mass flow rates are more effective than the other effective ones.

To maximize the efficiency of a solar collector, the input water temperature of the collector should be close to ambient air temperature, and as the input temperature increases, efficiency decreases. As the inlet temperature increases, the output fluid temperature also increases, which, in turn, increases the efficiency. On the other hand, increasing the temperature of the input water means increasing the temperature of the fluid inside the collector, which increases the thermal drop; therefore, there is an optimal inlet water temperature observed for temperatures higher than that the effect of reduced efficiency due to excessive heat loss.

The thickness and the insulation were the other factors in the collector's efficiency. Obviously, with the increase of the insulation thickness, the heat dissipation dropped, the collector decreased, and efficiency increased. In addition, because the polyurethane heat transfer coefficient is less than glass fiber and shows better resistance to heat transfer from the adsorbent plate to the outside, the efficiency will increase.

Considering the collector performance in a closed circuit in the evening when the storage temperature increases due to no heat stored, the fluid inlet temperature to the collector will increase continuously. Increasing the temperature to a certain extent increases the efficiency.

Increasing the number of glass coatings or increasing the thickness of the glass cover reduces heat loss from the collector's surface. As a result, energy increases.

6. ACKNOWLEDGEMENT

Authors would like to thank the Payame Noor University for support this work.

REFERENCES

1. Bogaerts, W.F. and Lampert, C.M., "Materials for photo thermal solar-energy conversion", ***Journal of Materials Science***, Vol. 18, (1983), 2847-2875. (https://doi.org/10.1007/BF00700767).
2. Kalogirou, S., "Solar thermal collectors and applications", ***Progress In Energy and Combustion Science***, Vol. 30, (2004), 231-295. (https://doi.org/10.1016/j.pecs.2004.02.001).
3. Tian, Y. and Zhao, C.Y., "A review of solar collectors and thermal energy storage in solar thermal applications", ***Applied Energy***, Vol. 104, (2013), 538-553. (https://doi.org/10.1016/ j.apenergy.2012.11.051).
4. Abdolzadeh, M. and Mehrabian, M.A., "The optimal slope angle for solar collectors in hot and dry parts of Iran", ***Energy Sources, Part A***, Vol. 34, (2012), 519-530. (https://doi.org/10.1080/ 15567036.2011.576413).
5. Riffat, S., Zhao, X. and Doherrty, P.S., "Developing a theoretical model to investigate thermal performance of a thin membrane heat-pipe solar collector", ***Applied Thermal Engineering***, Vol. 25, (2005), 899-91. (https://doi.org/10.1016/j.applthermaleng. 2004.08.010).
6. Cruz-Peragon, F., Palomar, J.M., Casanova, P.J., Dorado, M.P. and Manzano-Agugliaro, F., "Characterization of solar flat plate collectors", ***Journal of Science Direct***, April (2012), 1709–1720. (https://doi.org/10.1016/j.rser.2011.11.025).
7. Esen, M. and Esen, H., "Experimental investigation of a two-phase closed thermo syphon solar water heater", ***Solar Energy***, Vol. 79, (2005), 459-468. (https://doi.org/10.1016/j.solener. 2005.01.001).
8. Yousefi, T., Veysi, F., Shojaeizadeh, E. and Zinadini, S., "An experimental investigation on the effect of Al_2O_3-H_2O nanofluid on the efficiency of flat plate solar collector", ***Renewable Energy***, Vol. 39, (2012), 293-298. (https://doi.org/10.1016/ j.renene.2011.08.056).
9. Chen, Z., Furbo, S., Perers, B., Fan, J. and Andersen, E., "Efficiencies of flat plate solar collectors at different flow rates", ***Energy Procedia***, Vol. 30, (2012), 65-72. (https://doi.org/ 10.1016/j.csite.2016.08.006).
10. Kalogirou, S., "Prediction of flat plate collector performance parameters using artificial neural networks", ***Solar Energy***, Vol. 80, (2006), 248-259. (https://doi.org/10.1016/j.solener. 2005.03.003).
11. Kumar, N., Chavda, T. and Mistry, H.N., "A truncated pyramid non tracking type multipurpose solar cooker/hot water system", ***Applied Energy***, Vol. 87, (2010), 471-477. (https://doi.org/ 10.1016/j.apenergy.2009.06.031).
12. Ayompe, L.M. and Duffy, A., "Analysis of the thermal performance of a solar water heating systemwith flat plate collectors in a temperate climate", ***Applied Thermal Engineering***, Vol. 58, (2013), 447-454. (https://doi.org/ 10.1016/j.applthermaleng.2013.04.062).
13. Tyagi, H., Phelan, P. and Prasher, R., "Predited efficiency of a low-temperature nanfluid-based direct absorption solar collector", ***Journal of Solar Energy Engineering***, Vol. 131, (2009), 1-7. (https://doi.org/10.1063/1.3429737).
14. Taylor, R.A., Phelan, P.E., Otanicar, T.P., Walker, C.A., Nguyen, M., Trimble, S. and Prasher, R., "Applicability of nanofluids in high flux solar collectors", ***Journal of Renewable and Sustainable Energy***, Vol. 3, (2011), 023104. (https://doi.org/10.1063/1.3571565).
15. Choi, S. and Zhang, Z.G., "Anomalous thermal conductivity enhancement in nanotube suspensions", ***Applied Physics Letter***, Vol. 79, (2001), 2252-2254. (https://doi.org/10.1063/1.1408272).
16. Otanicar, T., Phelan, P., Parsher, R., Rosengarten, G. and Taylor, R., "Nanofluid-based direct absorption solar collector", ***Journal of Renewable and Sustainable Energy***, Vol. 2, (2010), 033102. (https://doi.org/10.1186/1556-276X-6-225).
17. Otanicar, P. and Golden, J., "Comparative environmental and economic analysis of conventional and nanofluid solar hot water technologies", ***Environmental Science and Technology***, Vol. 43, (2009), 6082-6087. (https://doi.org/10.1021/es900031j).
18. Rajabi Khanghahi, A., Zamen, M., Soufari, M., Amidpour, M. and Abbas Nejad, A., "Theoretical investigation of consumption patterns effect on optimal orientation of collector in solar water heating system", ***Journal of Renewable Energy and Environment (JREE)***, Vol. 4, No. 1, (2017), 1-10.
19. Mahian, O., Kianifar, A., Sahin, A. and Wongwises, S., "Performance analysis of a minichannel-based solar collector using different nanofluids", ***Energy Conversion and Management***, Vol. 88, (2014),129-138. (https://doi.org/10.1016/ j.enconman.2014.08.021).
20. Zamzamian, S., Keyanpour Rad, M., Kiani Neyestani, M. and Jamal-Abad, M.T., "An experimental study on the effect of Cu-synthesized/EG nanofluid on the efficiency of flat-plate solar collectors", ***Renewable Energy***, Vol. 71, (2014), 658-664. (https://doi.org/10.1016/j.renene.2014.06.003).
21. Jamal-Abad, M.T., Zamzamian, A., Imani, E. and Mansouri, M., "Experimental study of the performance of a flat-plate collector using Cu-water nanofluids", ***Journal of Thermophysics and Heat Transfer***, Vol. 27, (2013), 756-760. (https://doi.org/ 10.2514/1.T4074).
22. Mousazaeh, H., "A review of principal and sun-tracking methods for maximizing solar systems output", ***Renewable and Sustainable Energy Reviews***, Vol. 13, (2009), 1800-1818. (https://doi.org/10.1016/j.rser.2009.01.022).
23. Noghrehabadi, A., Hajidavaloo, E. and Moravej, M., "An experimental investigation of a 3-D solar conical collector performance at different flow rates", ***Journal of Heat and Mass Transfer Research***, Vol. 1, (2016), 57-66. (https://doi.org/ 10.22075/JHMTR.2016.477).
24. Bakir, O., "Experimental investigation of a spherical solar collector", Thesis submitted to the graduate School of Natural and Applied Science of Middle East Technical University, (April 2006).
25. Iljins, U. and Ziemelis, I., "Forecast of energy received by solar collectors", ***Proceedings of The International Scientific Conference Applied Information and Communication Technologies***, Jelgava, Latvia University of Agriculture, (2008), 62-67.
26. Iljins, U. and Ziemelis, I., "Theoretical calculation of energy received by semi-spherical solar collector", Latvia University of Agriculture, Liela str. 2, Jelgava, LV3000.
27. Shamim, M.A., Remesan, R., Han, D.-W., Ejaz, N. and Elahi, A., "An improved technique for global solar radiation estimation using numerical weather prediction", ***Journal of Atmospheric and Solar-Terrestrial Physics***, Vol. 129, (2015), 13-22. (https://doi.org/10.1016/j.jastp.2015.03.011).

28. Yousefi, T., Shojaeizadeh, E., Veysi, F. and Zinadini, S., "An experimental investigation on the effect of MWCNT-H_2O nanofluid on the efficiency of flatplate solar collectors", ***Experimental Thermal and Fluid Science***, Vol. 39, (2012), 207-212. (https://doi.org/10.4172/fundamentals-renewable-energy.1000200).
29. Do Ango, A.M., Medale, M. and Abid, C., "Optimization of the design of a polymer flat plate solar collector", ***Solar Energy***, Vol. 87, (2013), 64-75. (https://doi.org/10.1016/j.solener. 2012.10.006Get rights and content).
30. Cristofari, C., Notton, G., Poggi, P. and Louche, A., "Modelling and performance of a copolymer solar water heating collector", ***Solar Energy***, Vol. 72, (2002), 99-112. (https://doi.org/10.1016/ S0038-092X(01)00092-5).
31. Sen, Z., Solar energy fundamentals and modeling techniques, Springers, (2008).
32. Mohammadi, K. and Khorasanizadeh, H., "A review of solar radiation on vertically mounted solar surfaces and proper azimuth angles in six Iranian major cities", ***Renewable and Sustainable Energy Reviews***, No. 47, (2015), 504-518. (https://doi.org/10.1016/j.rser.2015.03.037).
33. ASHRAE Standard 93-86, Methods of testing and determine the thermal performance of solar collectors, ASHRAE, Atlanta (2003).
34. Duffie, J.A. and Beckman, W.A., Solar engineering of thermal processes, 4th Ed., Wiley, New York, (2013).
35. Rojas, D., Beermann, J., Klein, S. and Reindl, D., "Thermal performance testing of flat plate collectors", ***Solar Energy***, Vol. 82, (2008), 746-757. (https://doi.org/10.1016/j.solener. 2008.02.001).
36. Abernethy, R., Benedict, R. and Dowdell, R., "ASME measurement uncertainty", ***ASME paper***, (1983), 83-WA/FM-3.
37. Ma, J., Sun, W., Ji, J., Zhang, Y., Zhang, A. and Fan, W., "Experimental and theoretical study of the efficiency of a dual-function solar collector", ***Applied Thermal Engineering***, Vol. 31, (2011), 1751-1756. (https://doi.org/10.1016/ j.applthermaleng.2011.02.019).
38. Tongtuama, Y., Ketjoya, N., Vaivudha, S. and Thanaraka, P., "Effect of the diffuse radiation reflection from exterior wall on shading device integrated photovoltaic case of Thailand building", ***Energy Procedia***, No. 9, (2011), 104-116. (https://doi.org/10.1016/j.egypro.2011.09.012).
39. Boland, J., Huang, J. and Ridley, B., "Decomposing global solar radiation into its direct and diffuse components", ***Renewable and Sustainable Energy Reviews***,Vol. 28, (2013), 749-756. (https://doi.org/10.1016/j.rser.2013.08.023).
40. Goudarzi, K., Asadi Yousef-Abad, S., Shojaeizadeh, E. and Hajipour, A., "Experimental investigation of thermal performance in an advanced solar collector with spiral tube", ***International Journal of Engineering-Transactions A: Basics***, Vol. 27, (2013), 1149.
41. Ranjbar, S. and Seyyedvalilu, M., "The effect of geometrical parameters on heat transfer coefficient in helical double tube exchangers", ***Journal of Heat and Mass Transfer Research (JHMTR)***, Vol. 1, (2014), 75-82. (https://doi.org/10.22075/ JHMTR.2014.182).